Pharm Res
https://doi.org/10.1007/s11095-021-03042-8

RESEARCH PAPER

Pharmaceutical Excipients Enhance Iron-Dependent Photo-Degradation in Pharmaceutical Buffers by near UV and Visible Light: Tyrosine Modification by Reactions of the Antioxidant Methionine in Citrate Buffer

Natalia Subelzu [1,2] • Christian Schöneich [1]

Received: 4 January 2021 / Accepted: 5 April 2021

ABSTRACT

Purpose To evaluate the effect of excipients, including sugars and amino acids, on photo-degradation reactions in pharmaceutical buffers induced by near UV and visible light.

Methods Solutions of citrate or acetate buffers, containing 1 or 50 μM Fe^{3+}, the model peptides methionine enkephalin (MEn), leucine enkephalin (LEn) or proctolin peptide (ProP), in the presence of commonly used amino acids or sugars, were photo-irradiated with near UV or visible light. The oxidation products were analyzed by reverse-phase HPLC and HPLC-MS/MS.

Results The sugars mannitol, sucrose and trehalose, and the amino acids Arg, Lys, and His significantly promote the oxidation of peptide Met to peptide Met sulfoxide. These excipients do not increase the yields of hydrogen peroxide, suggesting that other oxidants such as peroxyl radicals are responsible for the oxidation of peptide Met. The addition of free Met reduces the oxidation of peptide Met, but, in citrate buffer, causes the addition of Met oxidation products to Tyr residues of the target peptides.

Conclusions Commonly used excipients enhance the light-induced oxidation of amino acids in model peptides.

KEY WORDS excipients · near UV and visible light · pharmaceutical peptides and proteins · photo-degradation · photo-Fenton reaction

ABBREVIATIONS

ABTS	2,2′-azino-bis(3-ethylebenzothiazole-6-sulfonic acid) diammonium salt
Arg	Arginine
DTPA	Diethylenetriaminepentaacetic acid
EDTA	Ethylenediaminetetraacetic acid
FA	Formic acid
Gly	Glycine
His	Histidine
HPLC	High-performance liquid chromatography
HRP	Horseradish peroxidase
LC	Liquid chromatography
LEn	Leucine enkephalin
Leu	Leucine
Lys	Lysine
mAbs	Monoclonal antibodies
MEn	Methionine enkephalin
Met	Methionine
MS	Mass spectrometry
Phe	Phenylalanine
ProP	Proctolin peptide
Q-TOF	Quadrupole time of flight
TFA	Trifluoroacetic acid
Thr	Threonine
t_R	Retention time
Tyr	Tyrosine
UV	Ultraviolet

INTRODUCTION

Pharmaceutical proteins and peptides are susceptible to light-induced degradation (1–3). The wavelengths of light that pharmaceutical products are exposed to vary between visible and near UV light, which some authors refer to as ambient light (4, 5). Amino acid residues do not significantly absorb near UV or visible light, except for some oxidation products of

✉ Christian Schöneich
schoneic@ku.edu

[1] Department of Pharmaceutical Chemistry, University of Kansas, 2095 Constant Avenue, Lawrence, Kansas 66047, USA

[2] Present address: Merck & Co., Inc, Rahway, NJ, USA

Published online: 21 April 2021

Trp residues, e.g. N-formylkynurenine, kynurenine, and 3-hydroxykynurenine (6–9). The exposure of proteins to ambient light can occur during manufacturing, packaging, visual inspection of products, storage, and patient administration (5, 10–13). Such light exposure can induce protein degradation, including the formation of post-translational modifications and aggregates (4, 5). As a potential consequence of such type of modifications, several side effects have been reported, including the reduction of clinical efficacy or adverse immunogenic responses (14–17). There are also reports of aesthetic changes in drug products, such as cloudiness, change of color, or the formation of visible particles (18–22).

Mechanistically, the processes leading to protein photodegradation during near UV and visible light exposure are not well established. Recently, we evaluated pharmaceutical buffers for their propensity to promote oxidation mechanisms via the photo-Fenton reaction under near UV and visible light (23). Specifically citrate buffer generated a variety of reactive species (Scheme 1), leading to multiple oxidation products of Met- and Tyr-containing model peptides, while acetate and succinate promoted only the formation of Met sulfoxide (23). Here, we have extended our studies to the role of additional excipients, specifically sugars and amino acids, in oxidation reactions induced by near UV and visible light in pharmaceutical buffers.

In order to design a stable formulation with an adequate shelf life, it is frequently necessary to add multiple excipients to formulations (24). These excipients function to improve the physical and chemical characteristics of the drug and constitute a vehicle for drug delivery (25). Studies have demonstrated that a combination of excipients can have a synergetic effect on the stabilization of formulations (26–28). However, some excipients are not inert and can afford changes in the stability of a formulation (23).

Excipients are classified with respect to their effects on formulations. For parenteral formulations, these categories are buffers, tonicifiers or osmolites, surfactants, solubilizers, preservatives, and stabilizing agents. Chelating agents (e.g., EDTA or DTPA) are frequently used to prevent oxidation promoted by transition metals. Moreover, amino acids and sugars or polyols are generally used to prevent aggregation, and/or oxidation (24).

Parenteral protein formulations are usually formulated in a pH range between 4 to 7, making the selection of buffer a critical factor. The most commonly used buffers are citrate, succinate, acetate, phosphate, tris(hydroxymethyl)aminomethane (Tris), Gly, and His (25, 29). The selection of buffer ultimately depends on the stability profiles of the respective proteins (26).

Sugars and amino acids, especially Arg, His, Gly, Lys, and Met, are commonly used stabilizers in parenteral formulations

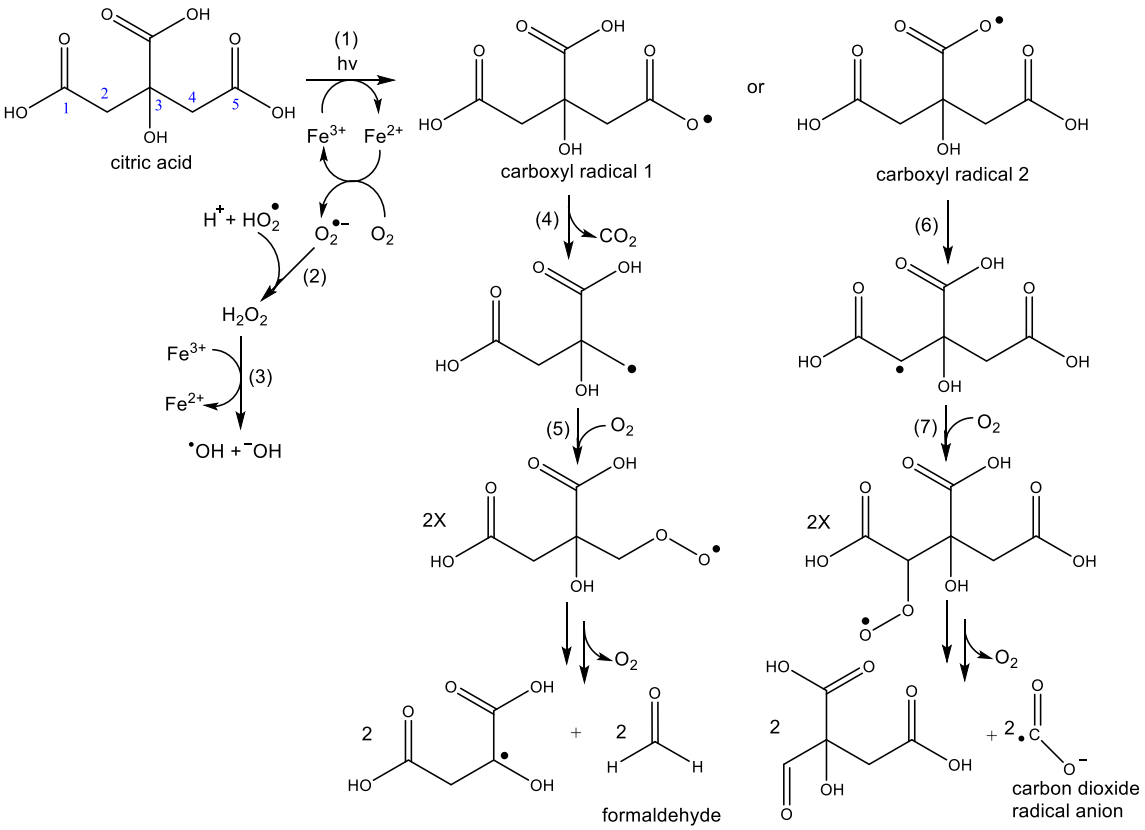

Scheme I Photo-Fenton reaction in citrate buffer.

(26), where positively charged amino acids can stabilize proteins by electrostatic interactions with acidic amino acid side chains (26, 30–35). However, Arg, Gly, and Lys can both stabilize or denaturate proteins, depending on their concentration and the nature of the proteins (30). Arg can increase protein solubility, and prevent protein unfolding and aggregation induced by heat or light (36). Lys tends to be less of a stabilizer compared to the other amino acids (30, 37). Met has been used as an antioxidant due to its ability to react with hydrogen peroxide (H_2O_2) and other reactive oxygen species (11, 28, 38).

Sugars stabilize proteins by increasing the protein-water potential, preferred hydration of proteins, and by increasing the activation energy for protein unfolding (39–41). Sugars also diminish protein aggregation during freeze-thaw and freeze-drying cycles (42, 43). However, depending on their structure, sugars can also promote protein degradation, for example via glycation (44).

Our data will show that amino acids and sugars can enhance the oxidative degradation of various model peptides (methionine- and leucine-enkephalin, and proctolin peptide) in iron-containing citrate and acetate buffer during the exposure of formulations to small doses of near UV or visible light. We selected iron concentrations of 1 and 50 μM, where 1 μM is in the range of iron levels reported for some formulations of monoclonal antibodies (1–9 μM) (45, 46), and 50 μM was selected for mechanistic purposes. The guideline for elemental impurities of the International Council for Harmonisation (ICH), ICHQ3D, sets no specific limits for the permitted daily exposure (PDE) to iron (47). We applied light doses between 9 and 35 Whm^{-2}, where 35 Whm^{-2} correpond to ca. 2 h exposure to UV A light of combined indoor lighting and window-filtered daylight in a home or clinical environment (48).

MATERIALS AND METHODS

Materials

Methionine enkephalin (MEn, YGGFM) and leucine enkephalin (LEn, YGGFL) were from Bachem (Bubendorf, Switzerland). Proctolin peptide (ProP, RYLPT) was from Genescript (Piscataway, NJ). Sodium citrate tribasic dihydrate, ferric chloride hexahydrate ($FeCl_3 \times 6\ H_2O$), sodium acetate anhydrous, $^{13}C_5$-L-methionine ($^{13}C_5$-L-Met), $^{13}C_2$-citric acid (C_2,C_4), ethylenediaminetetraacetic acid (EDTA), $^{18}O_2$ (stable isotope-labeled oxygen, 97%), sodium borohydride ($NaBH_4$), catalase from bovine liver, horseradish peroxidase (HRP), sucrose, D-mannitol, D(+)-trehalose, L-histidine (L-His) monochloride monohydrate, L-arginine (L-Arg) hydrochloride, and L-glycine (L-Gly) were purchased from Sigma (Saint Louis, MO). Diethylene-triaminepentaacetic acid (DTPA), L-lysine (L-Lys) hydrate, and L-methionine (L-Met) were purchased from Aldrich (Milwaukee, WI). 2,2′-Azino-bis (3-ethylebenzothiazole-6-sulfonic acid) diammonium salt (ABTS) was from Fluka (Saint Louis, MO). All chemicals used were analytical grade.

Peptide Photo-Irradiation

Solutions were prepared at a final volume of 400 μL, containing 500 μM peptide in water or 10 mM buffer (unless other specified concentration), pH 6.0, 1.0 or 50 μM Fe^{3+}, and either 50 mM amino acids or 120 mM sugars. Photo-irradiation was performed in a Rayonet© reactor (The Southern New England Ultraviolet Company, Branfort, CT), using near UV (RPR-3500 Å, $\lambda_{max} = 350$ nm; bandwidth 305–416 nm) or visible light lamps (RPR-4190 Å, $\lambda_{max} = 419$ nm; bandwidth 380–480 nm).

HPLC Analysis

The analysis of the oxidation products was achieved by reverse-phase HPLC. The photo-irradiated solutions (50 μL) were injected onto a C18 Vydac column (250 mm, I.D. 4.6 mm, 5 μm; Grace, Columbia, MD), maintained at 35°C in a column heater (CTO-20A; Shimadzu, Columbia, MD). Mobile phase A was 0.1% TFA in water, and mobile phase B consisted of acetonitrile with 0.1% TFA. The separation of the oxidation products was performed with a linear gradient changing mobile phase B from 7% to 35% within 30 min, delivered by two pumps (LC-20AT; Shimadzu, Columbia, MD), and the elution was monitored with a UV-detector (SPD-10Av; Shimadzu, Columbia, MD) set at $\lambda = 214$ nm.

HPLC-MS/MS Analysis

The HPLC-MS instrument consisted of a nanoAcquity UPLC coupled to a Xevo Q-TOF mass spectrometer (Waters Corp, Milford, MA). Mobile phase A was 0.1% formic acid in water, and mobile phase B was acetonitrile containing 0.1% formic acid (FA). Solutions of the photo-irradiated peptides were diluted in water containing 0.1% FA, and 2 μL were injected onto a CSH C18 nanocolumn (150 mm, I.D. 75 μm, Waters Corp, Milford, MA). Separation of the products was performed with a linear gradient increasing mobile phase B from 10 to 40% within 30 min. The MS^e data were acquired within a mass range between 50 to 2000 Da, with a ramp collision energy from 20 to 30 V and the cone voltage was set at 40 V. Data analysis was achieved with the MassLynx™ Software (Waters Corp; Milford, MA).

Detection of H_2O_2

Solutions of 600 μL, containing water or 10 mM buffer, pH 6.0, 1 or 50 μM Fe^{3+}, and either 50 mM amino acids or

120 mM sugars, were photo-irradiated with near UV lamps (RPR-3500 Å, λ_{max} = 350 nm, 9.7 Whm^{-2}) in a Rayonet© reactor. Aliquots (50 μL) were drawn before and after photo-irradiation. The aliquots were placed in a 96 well plate and were incubated in the dark for 10 min, after the addition of 5 μL of water or an aqueous solution containing 0.75 mg mL^{-1} of catalase. The H_2O_2 concentration was measured by the addition of 300 μL of an aqueous solution of ABTS (final concentration 0.5 mM) and HRP (final concentration 10 μg mL^{-1}) (49). The absorbance of the solutions was measured at λ = 415 nm in a plate reader (Infinite M200 Pro Tecan; Mannedorf, Switzerland) maintained at 25°C. The absorbance readings were compared with a calibration curve of standard solutions of H_2O_2 (0–100 μM) prepared in the respective buffers, for which the concentrations were separately measured by absorbance at λ = 240 nm ($\varepsilon_{H2O2,\ 240nm}$ = 43.6 M^{-1} cm^{-1}) (8).

RESULTS

Photo-Irradiation with near UV Light

Photo-Irradiation of MEn in the Presence of Amino Acids

Solutions of 500 μM MEn in either water, 10 mM acetate, or 10 mM citrate, pH 6.0, containing 1 or 50 μM Fe^{3+} and 50 mM amino acids, were photo-irradiated with near UV light (25.2 Whm^{-2}) in a Rayonet© reactor. Representative HPLC traces are displayed in Fig. 1. Control samples were prepared as described above and placed in the dark for 2 h (Fig. S1).

The photo-irradiation of MEn in citrate buffer containing 50 μM Fe^{3+} generated all the products which we described previously (23). Briefly, the first peak with a retention time (t_R) of 15.6 min corresponded to Met sulfoxide (product A) (Fig. 1a). The other products were three isomers of hydroxyphenylalanine (product B, peaks 2, 3 and 6; t_R = 16.9, 18.2 and 20.9 min, respectively), a modified Tyr residue with a mass increase of 28 Da, referred to as product C (peak 4, t_R = 20.1 min), and 3,4-dihydroxyphenylalanine (product D, peak 5, t_R = 20.5 min). All these oxidation products from MEn are listed in Table I. The unmodified MEn eluted with t_R = 22 min and the MS/MS spectrum is shown in Fig. S2.

When 50 mM Gly were added to a solution containing 500 μM MEn in 10 mM citrate, pH 6.0, and 50 μM Fe^{3+}, photo-irradiation produced similar yields of products B, C, and D but significantly higher yields of product A (Fig. 1a, green trace). The addition of Arg, Lys, and His reduced the yields of products B, C, and D, and further increased the yields of product A (Fig. 1a, red, light blue, and blue traces). The addition of Met significantly lowered the yields of products A, B, C, and D, but a new peak with t_R = 28.5 min was observed (Fig. 1a, yellow trace). This product is referred to as product H (see below).

The photo-irradiation of citrate solutions containing 1 μM Fe^{3+} (Fig. 1b, black trace), led to the formation of products A, B, C, and D. While the yield of product A was higher, the yields of products B, C, and D were lower compared to those obtained with 50 μM Fe^{3+} (Fig. 1b, black trace). At 1 μM Fe^{3+}, the addition of Gly showed no increase in product yields over citrate alone (Fig. 1b, green trace). Arg and His significantly decreased the yields of products B, C, and D, while the yield of product A significantly increased (Fig. 1b, red and blue traces). Interestingly, 1 μM Fe^{3+} solutions containing Lys generated the highest yield of product A (Fig. 1b, light blue trace), and significant yields of two new products eluting with t_R 12.9 min and 14.2 min, referred to as product I (see below). These new products were also detected upon the addition of Gly and Arg but at lower yields. Met containing solutions showed no oxidation peaks, except for a small yield of product H (see insert in Fig. 1b).

In acetate buffer, containing 500 μM MEn and 50 μM Fe^{3+}, we observed low yields of product A as the only oxidation product (Fig. 1c, black trace). The addition of Gly and Arg resulted in a small increase in the yields of product A (Fig. 1c, green and red traces), while Lys and His caused a more significant increase in the yield of product A, where His revealed the highest yield (Fig. 1c, light blue, and blue traces). The addition of Met abolished all peptide oxidation products (Fig. 1c, yellow trace).

In acetate solutions containing 500 μM MEn and 1 μM Fe^{3+} we detected low yields of product A (Fig. 1d, black trace). Upon the addition of Gly, Arg, or His, the yields of product A increased (Fig. 1d, green, red, and blue traces, respectively). The addition of 50 mM Lys promoted the highest yields of product A, as well as the formation of two additional peaks with t_R 12.9 min and 14.2 min, corresponding to product I (Fig. 1 d, light blue trace). The addition of Met abolished all peptide oxidation products (Fig. 1d, yellow trace).

Similarly to acetate solutions, the photo-irradiation of MEn in water containing 50 μM Fe^{3+}, did not produce significant yields of oxidation products (Fig. 1e, black trace). However, the addition of Gly or Arg promoted the formation of product A (Fig. 1e, green and red traces), while Lys and His further increased the yields of product A. The addition of Met abolished all peptide oxidation products (Fig. 1e, yellow trace).

The photo-irradiation of MEn in water containing 1 μM Fe^{3+} resulted in no oxidation products (Fig. 1f, black trace). The addition of Gly or His generated slightly higher yields of product A (Fig. 1f, green and blue traces). However, the addition of Arg and especially Lys resulted in significantly higher yields of product A (Fig. 1f, light blue, and blue traces).

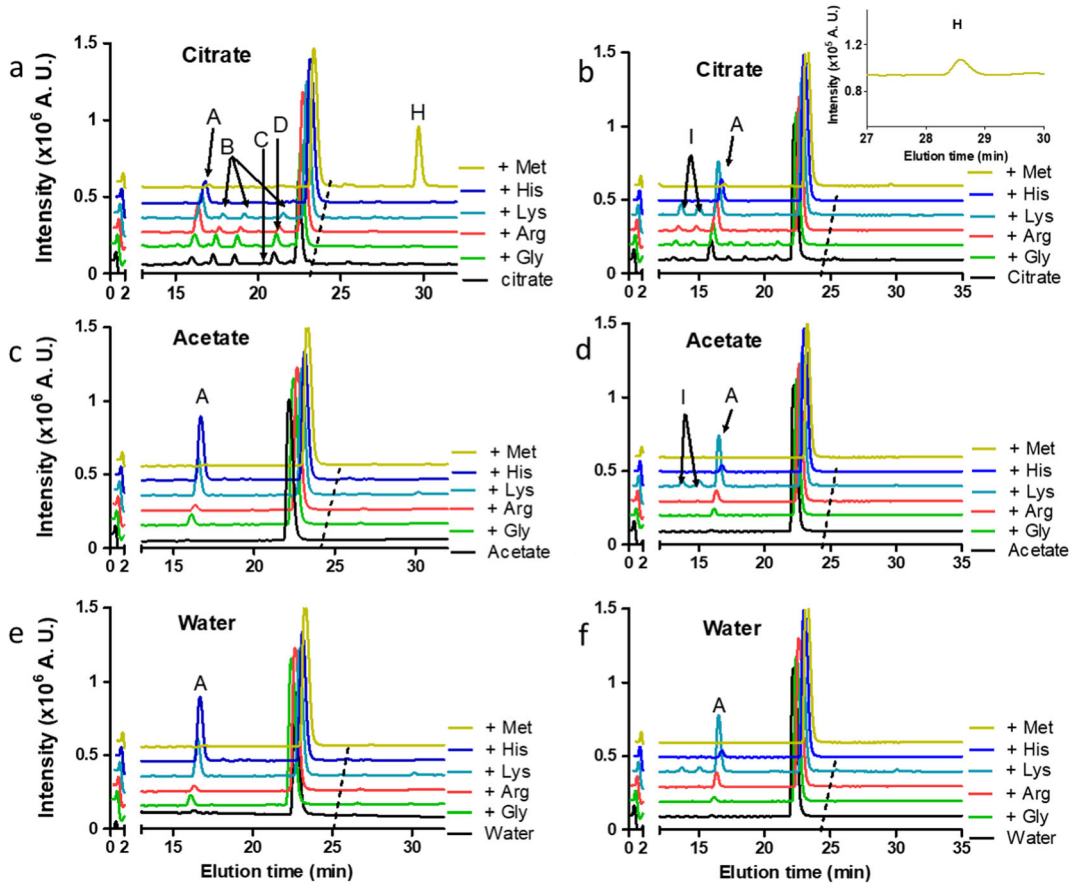

Fig. 1 Chromatograms of MEn photo-irradiated in solutions containing amino acids. Solutions of 500 μM of MEn were prepared in either water, 10 mM citrate, or 10 mM acetate, pH 6.0, containing 50 (a, c, and e) or 1 (b, d, and f) μM Fe^{3+} and no (black trace) or 50 mM amino acids: Gly (green), Arg (red), Lys (light blue), His (blue), or Met (yellow). Samples were photo-irradiated with near UV light (25.2 W h m^{-2}). HPLC chromatograms were monitored by UV detection at $\lambda = 214$ nm. Each trace represents the average of three independent experiments.

Moreover, the addition of Lys generated product I (Fig. 1d, light blue). In the presence of Met no peptide oxidation products were detected (Fig. 1f, yellow trace).

Table I Photoproducts of MEn

Product ID	t_R (min)	Sequence	m/z $[M+H]^+$
A	15.6	YGGFM(+16)	590.22
B	16.9, 18.2, 20.9	YGGF(+16)M	590.22
C	20.1	Y(+28)GGFM	602.22
D	20.5	Y(+16)GGFM	590.22
E	22.5	Y(+56)GGFM	630.27
F	23	Y(+114)GGFM	688.33
G	23	Y(+100)GGFM	674.31
H	28.5	Y(+38)GGFM(+48) [a]	660.30
I	12.9, 14.2	Y(+16)GGFM(+16)	606.18

[a] The initial modification of Tyr may be by 86 a.m.u., decomposing during mass spectrometry analysis leaving 38 a.m.u. at the Tyr residue and adding 48 a.m.u. to the C-terminal residue (see Discussion)

Characterization of Product H and Effect of Experimental Variables on the Formation of Product H

We photo-irradiated solutions containing 500 µM MEn in 10 mM citrate, pH 6.0, 50 mM Met and 50 µM Fe^{3+}, with near UV light (25.2 Whm^{-2}). HPLC-MS/MS analysis of product H revealed a molecular ion with m/z 660.29 (Fig. 2a), corresponding to a Δmass = 86 a.m.u. compared to the molecular ion of unmodified MEn (m/z = 574.3). An immonium ion of the N-terminal Tyr residue modified by the addition of 38 a.m.u. (Y + 38) was detected, and the addition of 38 a.m.u. was further corroborated by the ions b2, a2, b3, and b4. No ions were detected, which would indicate a product formed by the addition of 86 a.m.u. to the N-terminal Tyr residue. The Phe or Gly residues were not modified as indicated by the presence of the immonium ion of unmodified Phe, the b2, b3, and b4 ions, and the internal fragment GF. A fragment with m/z 612.28 was detected (Fig. 2a), which could be generated by the loss of 48 a.m.u. (consistent with the cleavage of CH_3SH) from the molecular ion (m/z = 660.29). Such a loss of 48 a.m.u. was not detected for unmodified MEn

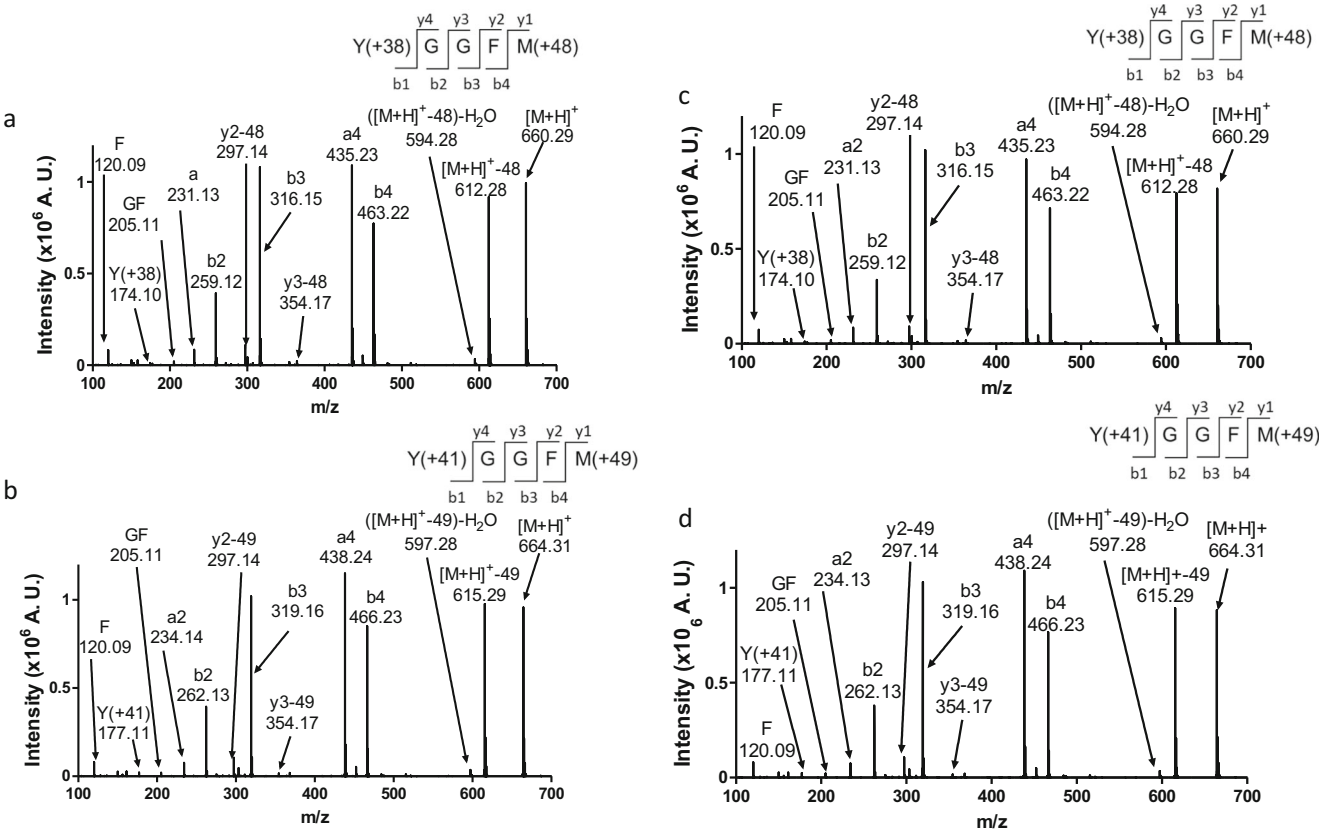

Fig. 2 MS/MS analysis of product H obtained in solutions containing combinations of ^{12}C- and ^{13}C-labeled citrate and Met. Solutions contained (a) ^{12}C-citrate and ^{12}C-Met, (b) $^{13}C_2$-citrate (C_2,C_4) and $^{13}C_5$-Met, (c) $^{13}C_2$-citrate (C_2,C_4) and ^{12}C-Met, and (d) ^{12}C-citrate and $^{13}C_5$-Met. Samples were photo-irradiated with near UV light (25.2 Whm^{-2}) and analyzed by HPLC-MS/MS.

(Fig. S2), indicating that modifications leading to product H were responsible for this fragmentation. Interestingly, small yields of fragment ions y2–48 and y3–48 were detected, suggesting an apparent addition of 48 a.m.u. to the C-terminal Met residue of MEn.

To evaluate whether the increase of 86 a.m.u. on MEn originated from the photo-degradation of citrate or Met, we employed $^{13}C_2$-citrate (C_2, C_4) and $^{13}C_5$-Met. Solutions were photo-irradiated with near UV light (25.2 Whm^{-2}) and analyzed by HPLC-MS/MS (Fig. 2b). We observed a molecular ion with m/z 664.31, indicating a mass increase of Δmass = 4 a.m.u. as compared to experiments with ^{12}C-citrate and ^{12}C-Met. The immonium ion of the modified N-terminal Tyr residue was detected with an m/z = 177.11 a.m.u, (Fig. 2b), which corresponded to an increase of 3 a.m.u. compared to the same immonium ion generated in experiments with ^{12}C-citrate and ^{12}C-Met. The ions b2, b3, and b4 ions showed an increase of 3 a.m.u. each, indicating that three carbons were incorporated into the modified Tyr residue. Further, we detected a fragment ion $[M + H]^+$-49, as compared to $[M + H]^+$-48 in experiments with ^{12}C-citrate and ^{12}C-Met, as well as the fragment ions y3–49 and y2–49, consistent with an increase of 1 a.m.u.

To evaluate which molecule was the source of the modifications, we photo-irradiated solutions of 500 μM MEn, containing 50 μM Fe^{3+} and a combination of either 10 mM $^{13}C_2$-citrate (C_2, C_4) and 50 mM ^{12}C-Met or 10 mM ^{12}C-citrate and 50 mM $^{13}C_5$-Met. We observed that photo-irradiation of solutions in $^{13}C_2$- citrate and ^{12}C Met resulted in a molecular ion with an m/z = 660.29 a.m.u, identical to the molecular ion obtained after of photo-irradiation in the presence of ^{12}C-citrate and ^{12}C-Met (Fig. 2c). When we changed the combination to $^{12}C_2$-citrate and $^{13}C_5$-Met we observed the molecular ion with m/z 664.31, revealing an increase by Δmass = 4 a.m.u. compared to ^{12}C-citrate and ^{12}C-Met (Fig. 2d). Once again, the ions containing the modified Tyr showed an increase of 3 a.m.u. while the fragment ions y3–49 and y2–49 are consistent with an increase of 1 a.m.u. at the C-terminus.

In a previous study (23), we demonstrated that •OH radicals, or their metal-bound equivalents/ hypervalent iron-oxo species (50), were produced during the photo-Fenton reaction and that these were responsible for the formation of oxidation products, including products B and D (23). To evaluate if these oxidants were involved in the formation of product H, we photo-irradiated solutions of 500 μM MEn, in 10 mM citrate, pH 6.0, 50 mM Met, and 50 μM Fe^{3+} containing

0.5, 1.0 and 2.0 M methanol, a scavenger of $^{\bullet}OH$ radicals. The presence of 0.5 M methanol (Fig. S3, red trace), reduced the yield of product H by 50% compared to the solution without added methanol (Fig. S3, yellow trace). A further increase in the concentration of methanol to 1.0 or 2.0 M (Fig. S3, blue and black traces, respectively), decreased the yield of product H to 33% of the original yield (Fig. S3), suggesting that $^{\bullet}OH$ radicals are necessary for the formation of product H.

The formation of product H showed a slight dependence on citrate concentrations between 1.0 and 75 mM, with a maximal yield around 50 mM citrate (Fig. S4a). No significant differences in the yields of product H were observed for Met concentrations between 25 mM and 100 mM, but slightly lower yields for 10 mM Met (Fig. S4b).

To evaluate whether atmospheric O_2 was involved in the formation of product H, solutions containing 500 μM MEn, in 10 mM citrate, pH 6.0, 50 mM Met and 50 μM Fe^{3+}, were first saturated with Ar for 30 min in the dark, and subsequently saturated with either $^{18}O_2$ or $^{16}O_2$ for 10 min. After photo-irradiation with near UV light (25.2 Whm^{-2}), HPLC-MS/MS analysis revealed the formation of the ion with m/z = 660.29 a.m.u. in solutions saturated with either $^{16}O_2$ or $^{18}O_2$ (Fig. S5a and b, respectively), indicating that atmospheric O_2 was not incorporated into product H. Moreover, in both solutions the immonium ions of modified Tyr showed an increase of 38 a.m.u., and identical fragment ions $[M + H]^+$-48, $([M + H]^+$-48)-H_2O, y3–48 and y2–48 were observed. .

To evaluate whether the amino group was converted into a Schiff base, photo-irradiated solutions containing 500 μM MEn, in 10 mM citrate, pH 6.0, 50 mM Met and 50 μM Fe^{3+} were subjected to reduction with 10 mM $NaBH_4$ for 20 min at room temperature in the dark. We observed no changes in the MS/MS spectrum (Fig. S6) compared to the non-reduced samples (Fig. 2a), indicating that the modified N-terminal Tyr residue did not contain a Schiff base.

We attempted to fractionate and enrich product H for analysis by NMR. However, MS analysis of the collected fraction revealed that product H decomposed during purification.

Photo-Irradiation of LEn in the Presence of Met

To evaluate if the C-terminal Met residue in MEn plays a role in product formation, we tested the formation of product H′ in LEn (here, product H′ differs from product H only with respect to the substitution of Met by Leu). Solutions of 500 μM LEn in 10 mM citrate, pH 6.0, containing 50 mM Met and 50 μM Fe^{3+} were photo-irradiated with near UV light (25.2 Whm^{-2}) and analyzed by HPLC-MS/MS. As for MEn, we observed a product characterized by a mass increase of Δmass = 86 a.m.u. compared to the unmodified LEn (Fig. S7). The MS/MS data showed some similarity to the pattern of MEn, i.e. the addition of 38 a.m.u. to the Tyr residue, corroborated by the immonium ion of the modified Tyr residue with m/z 174.09 a.m.u. and and the fragment ions a4 and b4, and fragments $[M + H]^+$-48 and $([M + H]^+$-48)-H_2O (Fig. S7a). However, in contrast to MEn we did not detect fragments y2–48 and y3–48 for LEn. No ion was observed indicating the addition of 86 a.m.u. to the Tyr residue. The photo-irradiation of LEn in the presence of ^{12}C-citrate and $^{13}C_5$-Met revealed the same pattern as for MEn (Figs. S7a and b).

Photo-Irradiation of ProP in the Presence of Met

An important question was whether photo-irradiation would lead to the modification of a Tyr residue which is neither located N- or C-terminal. For this, we prepared solutions of 500 μM ProP in 10 mM citrate buffer, pH 6.0, containing 50 mM Met and 50 μM Fe^{3+}. Solutions were photo-irradiated with near UV light (25.2 Whm^{-2}) and analyzed by HPLC-MS/MS. Photo-irradiation resulted in the formation of a new product (H*) with a molecular ion with m/z 735.39, consistent with the addition of 86 a.m.u. to ProP (Fig. S8a). The ions b2, a2, and b3, as well as the internal fragment Y(+38)L-CO (m/z 335.19) indicated that the addition of 86 a.m.u. occurred on the Tyr residue.

Experiments with $^{13}C_5$-Met resulted in the addition of 90 a.m.u. to the Tyr residue (Fig. S8b), consistent with the incorporation of four carbon atoms from Met, corroborated by the ions b2, b3, b4, y2, and y4.

Importantly, the molecular ions of modified ProP showed a neutral loss of 48 or 49, respectively, depending on whether photo-irradiation had been carried out in the presence of ^{12}C-Met or $^{13}C_5$-Met. However, no fragment was detected containing Tyr(+38) or Tyr(+41), as was the case for MEn and LEn. The differences between ProP on one hand and MEn and LEn on the other hand are likely caused by the location of Tyr, within the sequence vs. N-terminal, but potentially also by the Pro residue in ProP. ProP contains the Pro residue in the fourth position, restricting the flexibility of the backbone, as was previously demonstrated in peptides containing Pro in aqueous environments (51).

Photo-Irradiation of MEn in the Presence of Carbohydrates

We photo-irradiated solutions of 500 μM MEn, in 10 mM citrate, pH 6.0, containing 120 mM mannitol, sucrose or trehalose, and 50 μM Fe^{3+} with near UV light (25.2 Whm^{-2}). The oxidation products were analyzed by HPLC. The addition of mannitol increased the yields of product A, but significantly decreased the yields of products B, C, and D, compared to solutions without mannitol (Fig. 3a, green trace). The addition of sucrose led to higher yields of product A, as well as products E, F, and G (Fig. 3a, red trace). Product E, with t_R = 22.5 min, was characterized by the addition of 56 a.m.u. to Tyr. Products F and G coeluted at t_R = 23 min.

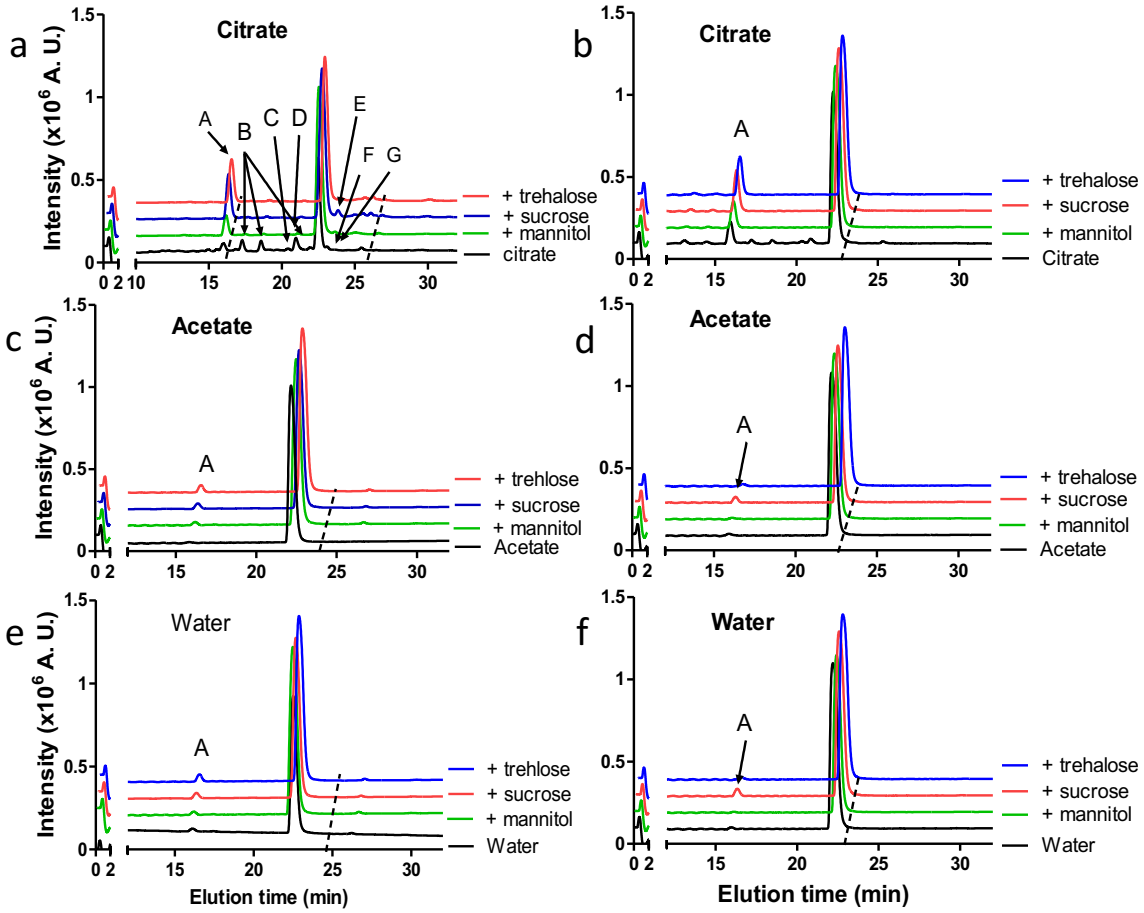

Fig. 3 Chromatograms of MEn photo-irradiated in solutions containing sugars. Solutions of 500 μM MEn were prepared in either water or 10 mM citrate or 10 mM acetate, pH 6.0, containing 50 (a, c, and e) or 1 (b, d, and f) μM Fe3+ without (black trace) or with added 120 mM mannitol (green), sucrose (red), or trehalose (blue). Samples were photoirradiated with near UV light (25.2 W h m-2). HPLC chromatograms were monitored by UV detection at λ = 214 nm. Each trace represents the average of three independent experiments.

Product F was characterized by the addition of 114 a.m.u. addition to the Tyr residue, while product G was characterized by the addition of 100 a.m.u. to the Tyr residue. Products G and F also form in the absence of sucrose when the concentration ratio of citrate:iron is >500 (23).

The addition of trehalose caused similar yields of product A as sucrose but increased the yields of products E, F, and G (Fig. 3, blue trace). Both sucrose- and trehalose-containing solutions decreased the yields of products B, C, and D with respect to the solution without sugars. As products B, C and D are generated via hydroxylation of MEn by $^{\bullet}$OH radicals (23), reduced yields of these products in the presence of large concentrations of carbohydrates are expected due to the competitive reaction of $^{\bullet}$OH radicals with the carbohydrates.

To evaluate the formation of oxidation products at lower concentrations of Fe^{3+}, we prepared solutions of 500 µM MEn in 10 mM citrate, pH 6.0, containing 1 µM Fe^{3+}. We observed a significant increase in the yields of product A in the presence of mannitol, sucrose, or trehalose (Fig. 3b, green, red, and blue traces, respectively), compared to citrate buffer without carbohydrates (Fig. 3b, black trace). However, products B, C, and D were not observed.

In acetate buffer, containing 50 µM Fe^{3+}, mannitol, sucrose, and trehalose promoted a slight increase in the yields of product A, compared to a solution without carbohydrates (Fig. 3c). No other oxidation products were detected. When the Fe^{3+} concentration was lowered to 1 µM Fe^{3+}, only sucrose promoted an increase in the yield of product A (Fig. 3d, red trace).

The photo-irradiation of solutions containing 500 µM MEn, 120 mM carbohydrates, 50 µM Fe^{3+}, and no buffer, demonstrated the formation of small yields of product A (Fig. 3e, green, red, and blue traces), while at 1 µM Fe^{3+}, product A was only generated in the presence of sucrose (Fig. 3f, red trace).

Formation of H_2O_2

We evaluated the photo-induced formation of H_2O_2 in water, 10 mM acetate or 10 mM citrate, pH 6.0, containing 1 or 50 µM Fe^{3+}, and 50 mM amino acids or 120 mM sugars.

Solutions of 10 mM citrate buffer, pH 6.0, containing 1 μM Fe^{3+} produced 98 μM H_2O_2 after photo-irradiation with a dose of 9.7 Whm^{-2} of near UV light (Fig. 4a, white column). A quantitative comparison of H_2O_2 yields in citrate buffer containing amino acids and sugars shows that, except for mannitol, all other excipients lowered the detectable yields of H_2O_2 (Fig. 4a) The specificity of the assay for H_2O_2 was evaluated by the addition of catalase (Fig. S9).

In 10 mM acetate or unbuffered water containing 1 μM Fe^{3+}, only low levels of H_2O_2 were detected (Figs. 4b and c). Notably the addition of Lys or His to water promoted the formation of small yields of H_2O_2 (Fig. 4c). When His was replaced by imidazole in water, slightly higher yields of H_2O_2 were generated (Fig. S10).

When the concentration of $Fe^{3+}$was increased to 50 μM, no significant levels of H_2O_2 were detected after photo-irradiation with 9.7 Whm^{-2} (Fig. S11). This observation is likely the result of reactions 1 and 3 (Scheme 1), where Fe^{3+} is involved in the formation and decomposition of H_2O_2. Higher concentrations of Fe^{3+} increase the transient levels of photo-generated Fe^{2+}, which react with H_2O_2 (23).

Importantly, especially in citrate buffer containing 1 μM Fe^{3+}, none of the additional excipients increased the levels of H_2O_2 (Fig. 4a), suggesting that H_2O_2 formation is not key to the formation of increased yields of product A in the presence of these excipients.

Formation of Oxidation Products by Peroxyl Radicals

Since the excipients did not promote an increase of H_2O_2 in citrate buffer, we decided to evaluate whether other oxidants could be responsible for the general increase in the formation of product A. A viable candidate would be the peroxyl radical, which forms by oxygen addition to carbon-centered radicals. For model studies, peroxyl radicals can be generated through the thermal decomposition of azo-initiators such as AAPH (52, 53). Therefore, 500 μM MEn in 10 mM citrate, pH 6.0, containing 50 μM Fe^{3+}, and different concentrations of AAPH (0 to 100 mM) were incubated at 37°C for 2 h and

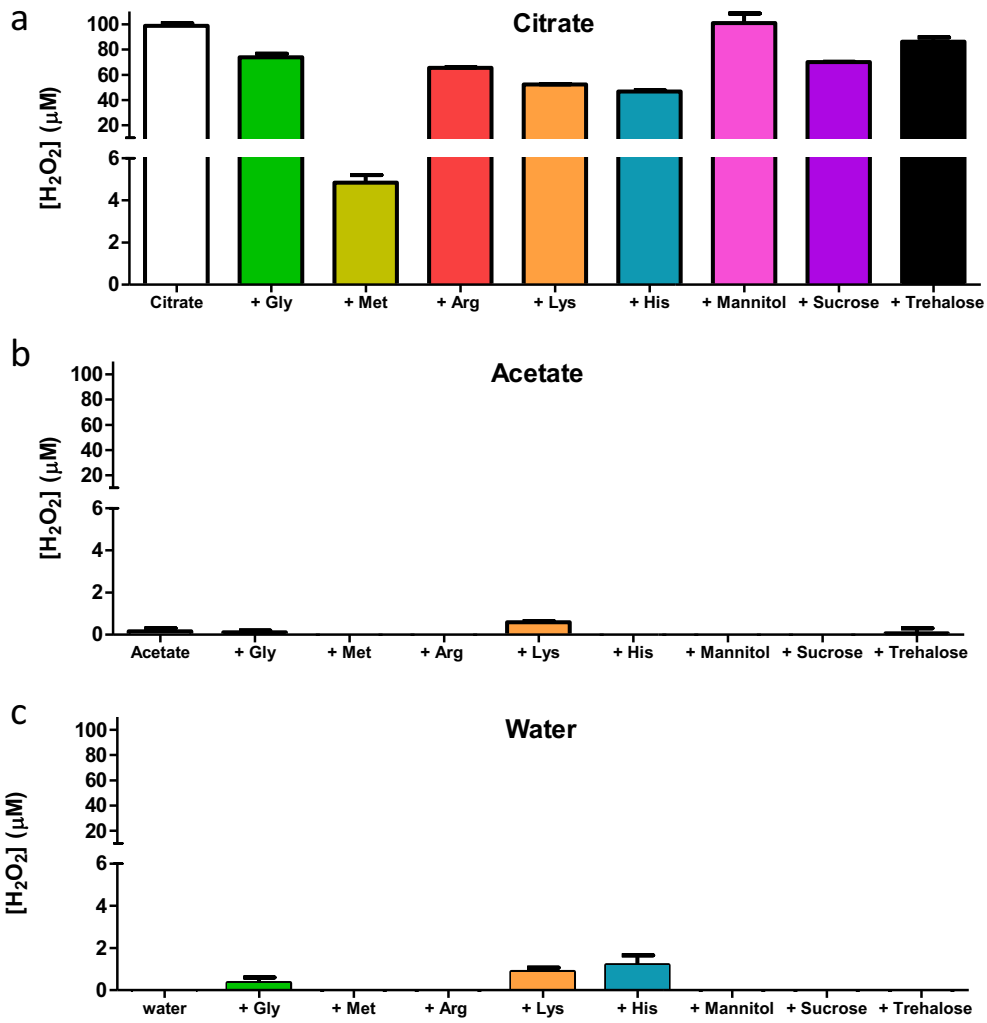

Fig. 4 Detection of H2O2 in solutions containing amino acids or sugars. Solutions of water, 10 mM citrate, or 10 mM acetate, pH 6.0, containing 1 μM Fe3+ were photo-irradiated with near UV light (9.7 Whm-2). Aliquots of 50 μL were taken after photo-irradiation, placed in a 96 well plate, and incubated with 5 μL of water or an aqueous solution containing 0.75 mg mL-1 catalase. After 10 min of incubation in the dark, 300 μL ABTS and HRP solution were added to each well and the absorbance was measured at λ = 415 nm in in plate reader (Infinite M200 Pro; Tecan, Mannedorf, Switzerland): (a) citrate buffer, (b) acetate buffer, and (c) water. Each column represents the average of three independent experiments.

the oxidation products were analyzed by HPLC with UV detection at λ = 214 nm (Fig. S12). Peroxyl radicals generated by the thermal decomposition of AAPH generated mainly product A, consistent with earlier studies on peroxyl radical reactions with organic sulfides (54), with yields depending on the initial AAPH concentration. The mechanism for the formation of peroxyl radicals from AAPH is shown in Fig. S12. Hence, peroxyl radical generation from excipients via the photo-Fenton reaction may play an important role in the formation of increased yields of product A.

Characterization of Product I

We observed the formation of two peaks with t_R = 12.9 min and 14.2 min, corresponding to product I (Table S1), during the photo-irradiation of solutions of 10 mM citrate (± 50 mM Gly, Arg, or Lys) (Fig. 1b) or acetate (+ 50 mM Lys) (Fig. 1d), pH 6.0, containing 500 μM MEn, and 1 μM Fe^{3+}. Product I was also generated in water containing 1 μM Fe^{3+} and 50 mM Lys (Fig. 1f).

The HPLC-MS/MS analysis detected molecular ions with m/z = 606.18 a.m.u. for both peaks with t_R = 12.9 min and 14.2 min (Figs. S13a and b, respectively), corresponding to the addition of 32 a.m.u. to MEn. The fragment ions b2, b3, b4, y1, y2, and y3 were consistent with the addition of 16 a.m.u. to each Tyr and Met, i.e. the formation of 3,4-dihydroxyphenylalanine and Met sulfoxide. The observation of two peaks with t_R = 12.9 and 14.2 min can be rationalized by the formation of Met sulfoxide diastereomers.

Photo-Irradiation with Visible Light

Photo-Irradiation of MEn in the Presence of Amino Acids and Sugars

Solutions of 500 μM MEn in 10 mM buffer, pH 6.0, containing 50 mM amino acids, and 1 μM Fe^{3+}, were photo-irradiated with 34.6 Whm^{-2} visible light and analyzed by HPLC.

Similar yields of product A were generated in citrate buffer alone and in citrate buffer containing 50 mM Gly or His. However, the addition of 50 mM Arg or Lys promoted the generation of higher yields of product A (Fig. 5a, red and light-blue traces, respectively). The photo-irradiation of solutions containing Met generated low yields of product H, as shown in the inset of Fig. 5a, yellow trace.

Also in acetate solutions we did not observe the formation of oxidation products in the absence of amino acids. However, the addition of Gly or Arg generated low yields of product A (Fig. 5b, green and red traces), while the addition of Lys significantly increased the yields of product A (Fig. 5b, light blue trace). No oxidation products were detected in the presence of

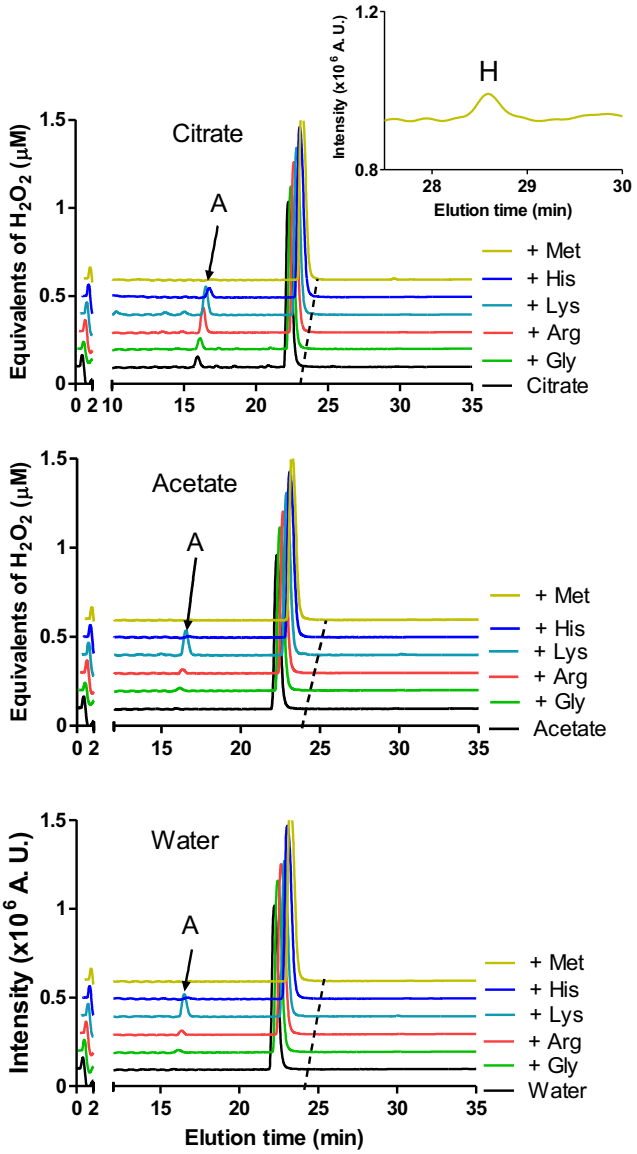

Fig. 5 Visible light photo-irradiation of MEn in the presence of amino acids. Solutions of 500 μM MEn in either water, 10 mM citrate, or 10 mM acetate, pH 6.0, containing 1 μM Fe^{3+} without (black trace) or with 50 mM Gly (green), Arg (red), Lys (light blue), His (blue), or Met (yellow) were photo-irradiated with visible light (34.6 Whm^{-2}), and analyzed by HPLC with UV detection at λ = 214 nm: (a) citrate, (b) acetate, and (c) water. Each trace represents the average of three independent experiments.

Met. Similar results were observed in water without added buffer (Fig. 5c), suggesting that the excipients are responsible for the generation of product A.

In addition, we monitored the generation of oxidation products in solutions containing sugars that were exposed to visible light (34.6 Whm^{-2}). Solutions of 500 μM MEn in 10 mM citrate, pH 6.0, containing 120 mM mannitol, sucrose, or trehalose displayed an increase in the yields of product A for all sugars with higher yields for sucrose and trehalose (Fig. 6a).

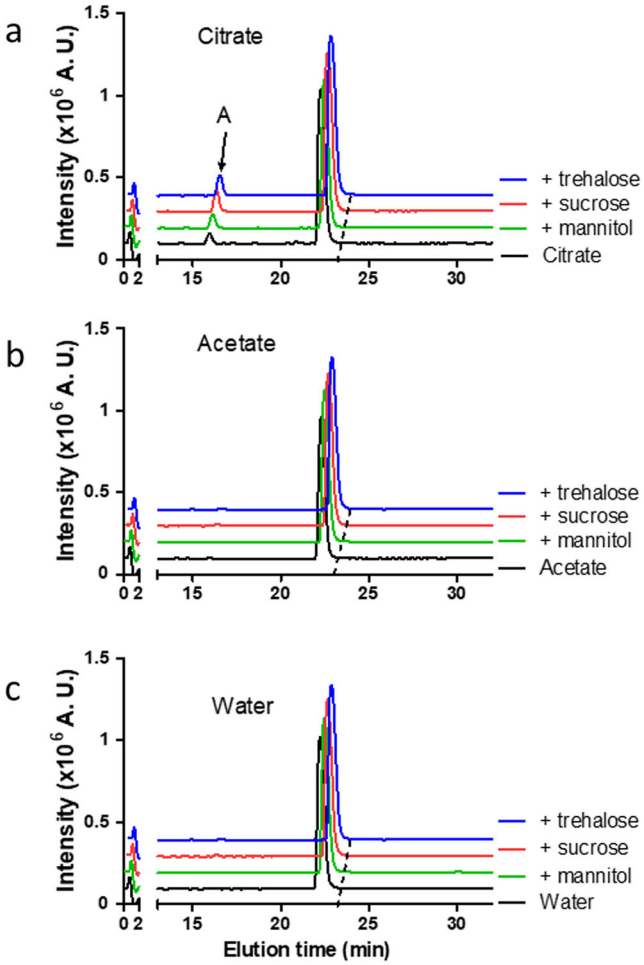

Fig. 6 Visible light photo-irradiation of MEn solutions in the presence of sugars. Solutions of 500 μM MEn were prepared in water or 10 mM citrate, or acetate pH 6.0, containing 1 μM Fe^{3+} without (black trace) or with added 120 mM sugars mannitol (green), sucrose (red), or trehalose (blue). Samples were photo-irradiated with visible light (34.6 Whm^{-2}), and analyzed by HPLC with UV detection at $\lambda = 214$ nm. (a) citrate, (b) acetate, and (c) water. Each treace represents the average of three independent experiments.

In contrast to citrate buffer, no significant yields of oxidation products were detected in either 10 mM acetate or water containing 1 µM Fe^{3+} and either mannitol, sucrose, or trehalose (Figs. 6b and c).

Combination of Excipients with EDTA or DTPA

Solutions containing 500 µM MEn, 10 mM citrate, pH 6.0, 120 mM sucrose, 50 mM amino acids, 50 µM Fe^{3+}, and 250 µM EDTA or DTPA, were photo-irradiated with near UV light (25.2 Whm^{-2}). After photo-irradiation, samples were analyzed by HPLC with UV detection ($\lambda = 214$ nm). When the added amino acid was Gly, we detected the formation of products A and E (Fig. 7, green traces), where the yield of product A was slightly higher in the presence of EDTA compared to DTPA. Similar yields of products A and E were also detected when the added amino acid was Lys (Fig. 6, orange traces). However, the addition of Met reduced the formation of product A but promoted the formation of product H. Moreover, products E, F, and G were detected (Fig. 7, grey and black traces).

DISCUSSION

The present work shows that commonly used excipients can promote or inhibit photo-degradation pathways in pharmaceutical buffers. Photo-degradation reactions were elucidated with model peptides as oxidation targets such as MEn, LEn, and ProP. In general, citrate promoted the oxidative degradation of these peptides via the photo-Fenton oxidation. The addition of selected amino acids (except Met) or carbohydrates (in citrate buffer) enhanced the oxidation yields specifically of Met sulfoxide (product A). The addition of Met largely prevented the photochemical formation of Met sulfoxide, but, in citrate buffer, resulted in the generation of a Tyr modification (product H). Mechanistic features of the photo-Fenton reaction in the presence of amino acids and carbohydrates will be discussed in the following.

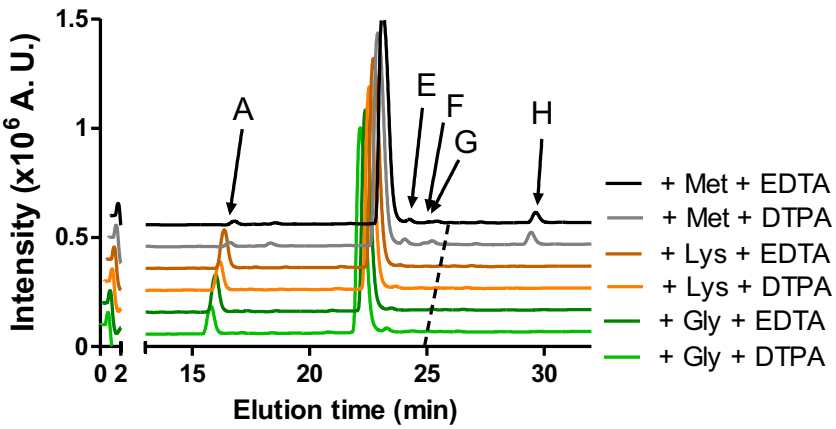

Fig. 7 MEn photo-irradiated in solutions containing a combination of excipients. Solutions of 500 μM of MEn in 10 mM citrate, pH 6.0, containing 1 μM Fe^{3+}, 120 mM sucrose, 50 mM Gly, Lys or Met, and 250 μM EDTA or DTPA, were photo-irradiated with near UV light (25.2 Whm^{-2}) and analyzed by HPLC with UV detection at $\lambda = 214$ nm.

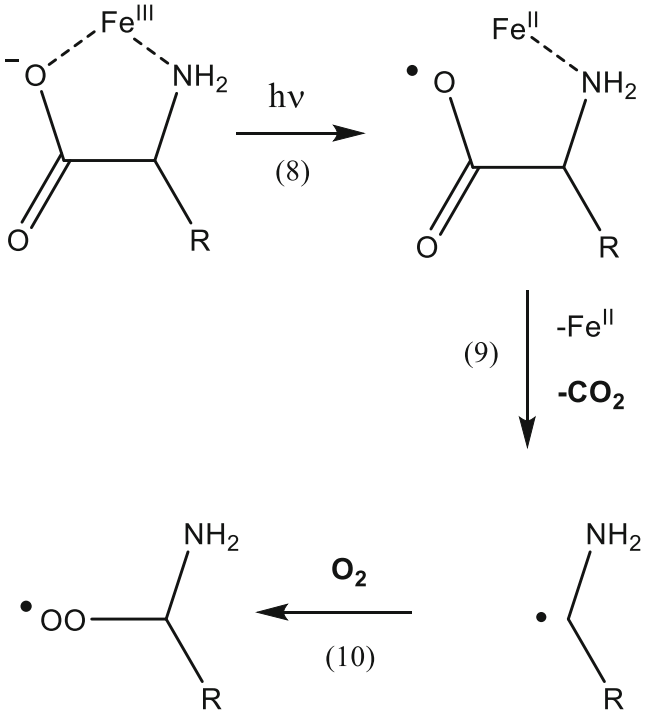

Scheme 2 Photo-induced peroxyl radical formation via LMCT in amino acid-Fe^{3+} complexes

Effect of Amino Acids

In citrate buffer, none of the added amino acids increased H_2O_2 formation (Fig. 4); however, except for Met, these excipients caused an increase of the yields of Met sulfoxide (product A). These data suggest that alternative oxidants are responsible for product A formation. Based on our studies with model peroxyl radicals from AAPH, we propose that amino acid-derived peroxyl radicals cause the increased yields of product A. Peroxyl radicals can be generated from the amino acids used in this study via (i) reaction with $^{\bullet}OH$ radicals (55) or (ii) via direct photo-induced ligand-to-metal charge transfer (LMCT) (56) within amino acid-iron complexes, followed by decarboxylation and the addition of oxygen to an intermediary α-amino radical (57). In citrate buffer, hydroxyl radicals are generated via reactions 1–3 (Scheme 1) (23). Specifically, Arg, Lys, and His provide multiple sites, for $^{\bullet}OH$ radical attack (58), where the ensuing carbon-centered radicals will subsequently add O_2 to yield peroxyl radicals. However, $^{\bullet}OH$ radical attack on amino acids cannot be the only mechanism to yield peroxyl radicals. This is evident from photo-Fenton oxidation reactions in acetate buffer or water, reaction media which do not generate products typical for $^{\bullet}OH$ radical reactions (23). Here, direct LMCT within amino acid-Fe^{3+} complexes (57) will lead to peroxyl radicals according to reactions 8–10, displayed in Scheme 2. Importantly, amino acids bind Fe^{3+} with high formation constants ($\log K > 8.0$) at acidic pH values ($pH \leq 3.35$) (59). These complexes represent chelates involving both the amino and the carboxylate groups (59), where binding to the metal promotes deprotonation of the amino group even at acidic pH (59, 60).

In general, the addition of Met prevented the generation of oxidation products from MEn, LEn and ProP. This is due to the efficient reaction of thioethers with reactive oxygen species such as hydrogen peroxide (61), peroxyl radicals (54) and hydroxyl radicals (62) which render Met a suitable antioxidant. In acetate buffer and water, no reactions of Met-derived products with our target peptides were observed. However, in citrate buffer an oxidation product of Met reacted with peptide Tyr residues, as discussed in more detail below.

Scheme 3 Reaction of trehalose peroxyl radicals with Met

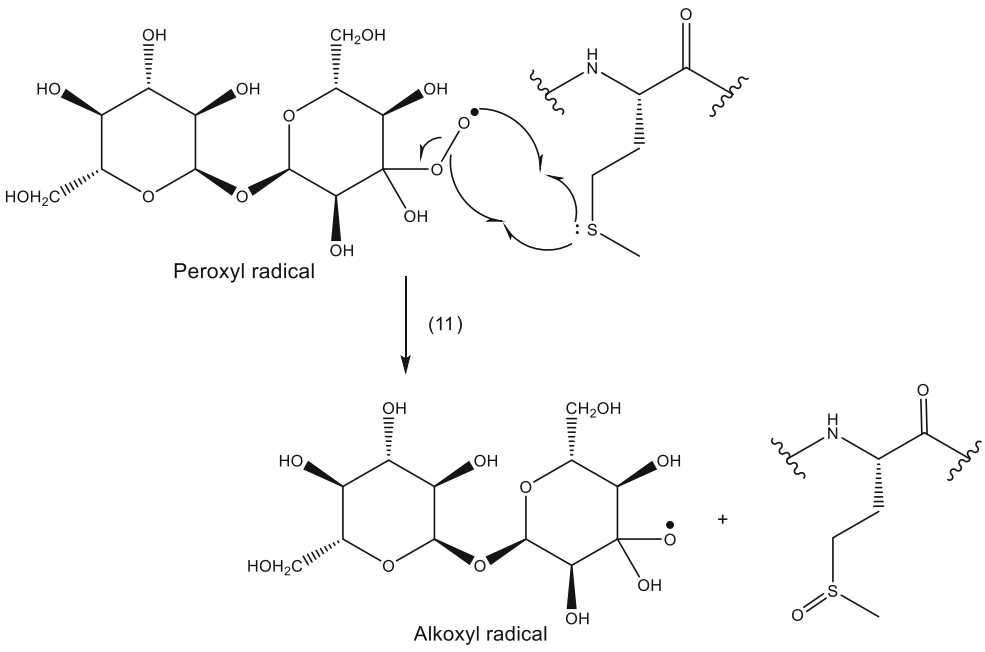

Scheme 4 Condensation of methional to Tyr

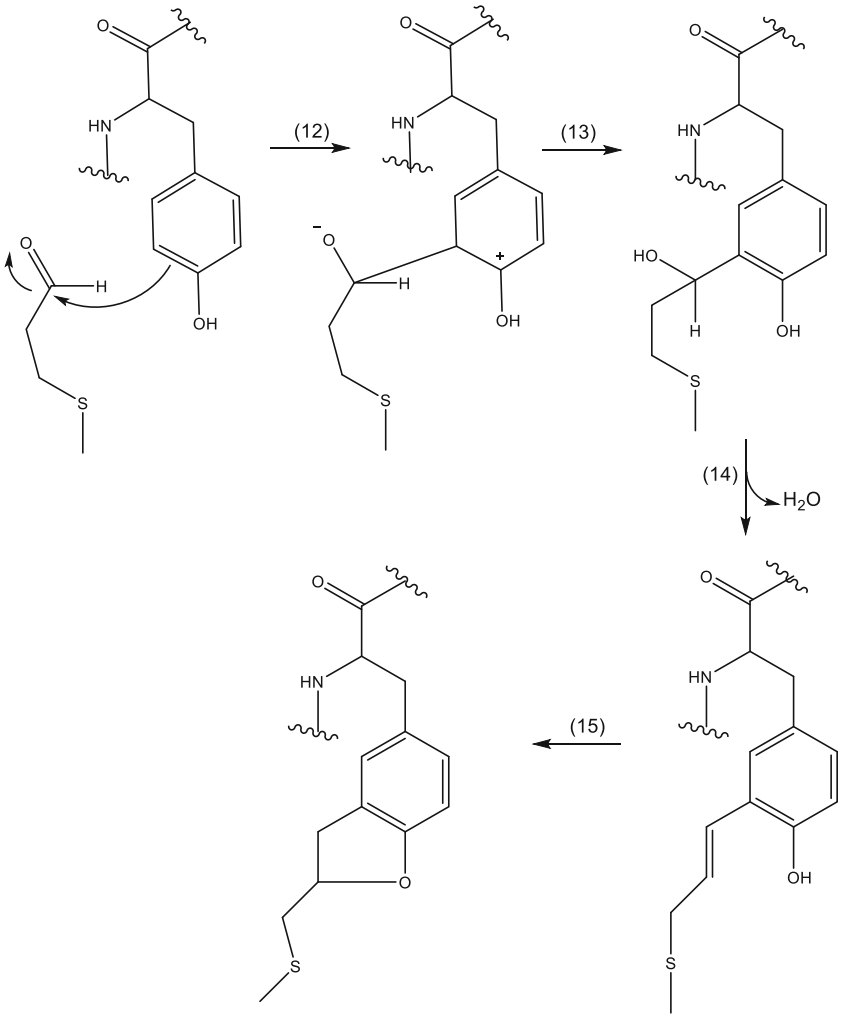

Effect of Sugars

The presence of sugars enhanced the formation of product A in citrate buffer, suggesting peroxyl radical formation via the reaction of hydroxyl radicals generated from citrate. Scheme 3 shows the reaction of a representative peroxyl radical from trehalose with Met. An important feature of the reaction of peroxyl radicals with organic sulfides is the generation of alkoxyl radicals (54), which are powerful oxidants and can carry out additional oxidation reactions.

Studies by Morelli et al demonstrated that the reactivity of the different sugars towards oxidation by $^{\bullet}OH$ radicals depended on the number of hydroxyl groups present in the sugar molecule, rendering disaccharides more reactive than monosaccharides (63). However, at the employed carbohydrate concentrations we expect that $^{\bullet}OH$ radicals react quantitatively with the carbohydrates. The enhanced yields of product A in the presence of sucrose and trehalose vs. mannitol (Fig. 3) are likely caused by different reactivities of the individual peroxyl radicals and/or secondary reactions of product radicals.

Specific Reactions of the Antioxidant Met in Citrate Buffer

Of specific interest is the modification of peptide Tyr residues when Met was present in citrate buffer. The photo-Fenton reaction generates various oxidants including H_2O_2 and $^{\bullet}OH$ radicals (Scheme 1). Obviously, H_2O_2 can react with free Met to generate Met sulfoxide, a product which we detected by HPLC-MS/MS analysis (data not shown). The $^{\bullet}OH$ radical represents a one-electron oxidant, which will initially add to the Met sulfur atom and trigger decarboxylation via an intermediary sulfur-oxygen three-electron bonded radical cation (62). The resulting α-aminoalkyl radical will react with oxygen and convert to 3-methylthiopropanal (methional) (64). Methional is also generated via riboflavin-photosensitized oxidation of Met (65). Methional can add to Tyr via phenol-aldehyde condensation (66, 67) (Scheme 4; reactions 12–15), which would lead to the net addition of 86 a.m.u. to the Tyr residue, as observed for ProP. It is possible that the phenolic hydroxyl group subsequently adds to the double bond, yielding a bicyclic product (reaction 15).

Methional contains four carbon atoms from the original Met residue (one carbon atom is lost during decarboxylation of the original Met). Hence, when ^{12}C-Met was replaced by $^{13}C_5$-Met during the photo-Fenton reaction, the phenol-aldehyde condensation with ProP caused a net addition of 90 a.m.u.

Interestingly, we did not detect any evidence for the addition of 86 (or 90) a.m.u. to the N-terminal Tyr residues in MEn and LEn. However, for the addition products from all peptides HPLC-MS/MS analysis detected a neutral loss of 48 (after photo-Fenton reaction in the presence of ^{12}C-Met) or 49 ($^{13}C_5$-Met) a.m.u., consistent with the elimination of CH_3SH. Specifically, for MEn and LEn we detected the products of such neutral losses, i.e. peptides containing Tyr(+38 a.m.u.). These data suggest that the aldehyde-phenol condensation products of especially N-terminal Tyr residues are unstable during positive electrospray ionization, and eliminate CH_3SH, potentially via reaction with the N-terminal amino groups. Interestingly, the fragment ions y2–48 and y3–48 of product H, detected when MEn was photo-irradiated in the presence of ^{12}C-Met, suggest that during MS analysis CH_3SH may somehow associate with the C-terminus of MEn. One could speculate about a gas phase addition to the C-terminal carboxylic acid of Met in MEn, generating a 2-(alkylamino)-1,4-bis(methylthio)butane-1,1-diol derivative, but such structure would certainly not be stable in aqueous solution. Because of the fragments y2–48 and y3–48 (or y2–49 and y3–49 when product H was generated from MEn in the presence of $^{13}C_5$-Met) the sequences of product H from MEn in Fig. 2 are given as Y(+38)GGFM(+48) and Y(+41)GGFM(+49), respectively. We have kept a similar notation for product H′ from LEn (Fig. S7), since we detected fragment ions containing Y(+38) and Y(+41), respectively.

We note that during the photo-sensitized oxidation of Met by riboflavin, methional was observed to undergo further degradation to CH_3SH and propenal (68). Technically, propenal could add to the Tyr residue, but a subsequent elimination of water to generate an addition product Tyr(+38) would be difficult. Moreover, no propenal adduct of ProP was detected.

Robustness of the Formulation

The literature offers some criteria regarding the acceptable yields of aggregation, oxidation, and charge variants present in a protein formulation (69). The excipients used should stabilize or ensure minimal modifications in pharmaceutics produced during manufacturing and storage, which is considered formulation robustness (70). Under our experimental conditions, an increase in the number of excipients (i.e., by addition of amino acids or carbohydrates, and EDTA or DTPA) used for protein formulation was not necessarily helpful to the stability of the model peptides, as demonstrated in Fig. 7. Especially the addition of EDTA or DTPA to protein formulations aims at reducing metal-catalyzed oxidation. However, even EDTA or DTPA chelates of iron are not necessarily redox-inert and can react with various substrates, including hydrogen peroxide (71–76). Moreover, in iron chelates of EDTA and DTPA the amino and carboxylate groups are amenable to LMCT analogous to the reactions shown for citrate in Scheme 1 and for amino acids in Scheme 2. Earlier we had shown that EDTA and DTPA were able to promote the photo-Fenton oxidation of MEn in acetate buffer (23). Hence, under conditions of light exposure EDTA and DTPA may enhance rather than prevent the oxidation of formulation constituents.

CONCLUSIONS

In citrate buffer, photo-Fenton processes lead to iron-dependent oxidative modifications of target peptides during the exposure to near UV and visible light. Here, the addition of selected excipients such as Arg, Lys, mannitol, sucrose or trehalose changes the product patterns, generating higher yields of Met sulfoxide. In acetate buffer or water, specifically the addition of Lys or His promote Met oxidation depending on the concentration of ferric iron. Not surprisingly, the addition of free Met protects the target peptides against photo-Fenton oxidation. However, in citrate buffer an oxidation product of free Met, methional, can modify peptide Tyr residues via a condensation reaction.

SUPPLEMENTARY INFORMATION

The online version contains supplementary material available at https://doi.org/10.1007/s11095-021-03042-8.

REFERENCES

1. Kerwin BA, Remmele RL Jr. Protect from light: photodegradation and protein biologics. J Pharm Sci. 2007;96(6):1468–79.
2. Hawe A, Wiggenhorn M, van de Weert M, Garbe JH, Mahler H-C, Jiskoot W. Forced degradation of therapeutic proteins. J Pharm Sci. 2012;101(3):895–913.
3. Schöneich C. Photo-degradation of therapeutic proteins: mechanistic aspects. Pharm Res. 2020;37(3):45.
4. Luis LM, Hu Y, Zamiri C, Sreedhara A. Determination of the acceptable ambient light exposure during drug product manufacturing for long-term stability of monoclonal antibodies. PDA J Pharm Sci Technol. 2018;72(4):393–403.
5. Sreedhara A, Yin J, Joyce M, Lau K, Wecksler AT, Deperalta G, et al. Effect of ambient light on IgG1 monoclonal antibodies during drug product processing and development. Eur J Pharm Biopharm. 2016;100:38–46.
6. Walrant P, Santus R, Grossweiner L. Photosensitizing properties of N-formylkynurenine. Photochem Photobiol. 1975;22(1–2):63–5.
7. Parker NR, Korlimbinis A, Jamie JF, Davies MJ, Truscott RJ. Reversible binding of kynurenine to lens proteins: potential

protection by glutathione in young lenses. Invest Ophthalmol Vis Sci. 2007;48(8):3705–13.
8. Razygraev A, Arutiunian A. Determination of human serum glutathione peroxidase activity, by using hydrogen peroxide and 5, 5′-dithio-bis (2-nitrobenzoic acid). Klin Lab Diagn. 2006;6:13–6.
9. Ávila F, Ravello N, Zanocco AL, Gamon LF, Davies MJ, Silva E. 3-Hydroxykynurenine bound to eye lens proteins induces oxidative modifications in crystalline proteins through a type I photosensitizing mechanism. Free Radic Biol Med. 2019;141:103–14.
10. Rathore A, Bhambure R, Ghare V. Process analytical technology (PAT) for biopharmaceutical products. Anal Bioanal Chem. 2010;398(1):137–54.
11. Shah DD, Zhang J, Maity H, Mallela KMG. Effect of photodegradation on the structure, stability, aggregation, and function of an IgG1 monoclonal antibody. Int J Pharm. 2018;547(1–2):438–49.
12. Patro SY, Freund E, Chang BS. Protein formulation and fill-finish operations. 2002.
13. Cromwell ME, Hilario E, Jacobson F. Protein aggregation and bioprocessing. AAPS J. 2006;8(3):E572–9.
14. Bessa J, Boeckle S, Beck H, Buckel T, Schlicht S, Ebeling M, et al. The immunogenicity of antibody aggregates in a novel transgenic mouse model. Pharm Res. 2015;32(7):2344–59.
15. Freedman MS, Pachner AR. Neutralizing antibodies to biological therapies: a "touch of gray" vs a "black and white" story. In: AAN Enterprises. 2007.
16. Calabresi P, Giovannoni G, Confavreux C, Galetta S, Havrdova E, Hutchinson M, et al. The incidence and significance of anti-natalizumab antibodies: results from AFFIRM and SENTINEL. Neurology. 2007;69(14):1391–403.
17. Br B, Bessa J, Folzer E, Ríos Quiroz A, Schmidt R, Bulau P, et al. Extensive chemical modifications in the primary protein structure of IgG1 subvisible particles are necessary for breaking immune tolerance. Mol Pharm. 2017;14(4):1292–9.
18. Doessegger L, Mahler H-C, Szczesny P, Rockstroh H, Kallmeyer G, Langenkamp A, et al. The potential clinical relevance of visible particles in parenteral drugs. J Pharm Sci. 2012;101(8):2635–44.
19. Carpenter JF, Randolph TW, Jiskoot W, Crommelin DJ, Middaugh CR, Winter G, et al. Overlooking subvisible particles in therapeutic protein products: gaps that may compromise product quality. J Pharm Sci. 2009;98(4):1201–5.
20. Du C, Barnett G, Borwankar A, Lewandowski A, Singh N, Ghose S, et al. Protection of therapeutic antibodies from visible light induced degradation: use safe light in manufacturing and storage. Eur J Pharm Biopharm. 2018;127:37–43.
21. Tønnesen HH. Formulation and stability testing of photolabile drugs. Int J Pharm. 2001;225(1–2):1–14.
22. Li Y, Polozova A, Gruia F, Feng J. Characterization of the degradation products of a color-changed monoclonal antibody: tryptophan-derived chromophores. Anal Chem. 2014;86(14):6850–7.
23. Subelzu N, Schöneich C. Near UV and visible light induce iron-dependent photo-degradation reactions in pharmaceutical buffers: mechanistic and product studies. Mol Pharm. 2020;17(11):4163–79.
24. Falconer RJ. Advances in liquid formulations of parenteral therapeutic proteins. Biotechnol Adv. 2019;37(7):107412.
25. Pramanick S, Singodia D, Chandel V. Excipient selection in parenteral formulation development. Pharma Times. 2013;45(3):65–77.
26. Wlodarczyk SR, Custódio D, Pessoa A Jr, Monteiro G. Influence and effect of osmolytes in biopharmaceutical formulations. Eur J Pharm Biopharm. 2018;131:92–8.
27. LeClair DA, Cranston ED, Xing Z, Thompson MR. Evaluation of excipients for enhanced thermal stabilization of a human type 5 adenoviral vector through spray drying. Int J Pharm. 2016;506(1–2):289–301.
28. Schöneich C. Redox processes of methionine relevant to β-amyloid oxidation and Alzheimer's disease. Arch Biochem Biophys. 2002;397(2):370–6.
29. Brange J, Havelund S, Hougaard P. Chemical stability of insulin. 2. Formation of higher molecular weight transformation products during storage of pharmaceutical preparations. Pharm Res. 1992;9(6):727–34.
30. Platts L, Falconer RJ. Controlling protein stability: mechanisms revealed using formulations of arginine, glycine and guanidinium HCl with three globular proteins. Int J Pharm. 2015;486(1–2):131–5.
31. Platts L, Darby SJ, Falconer RJ. Control of globular protein thermal stability in aqueous formulations by the positively charged amino acid excipients. J Pharm Sci. 2016;105(12):3532–6.
32. Jorgensen L, Hostrup S, Moeller EH, Grohganz H. Recent trends in stabilising peptides and proteins in pharmaceutical formulation–considerations in the choice of excipients. Expert Opinion on Drug Delivery. 2009;6(11):1219–30.
33. Chi EY, Krishnan S, Randolph TW, Carpenter JF. Physical stability of proteins in aqueous solution: mechanism and driving forces in nonnative protein aggregation. Pharm Res. 2003;20(9):1325–36.
34. Kamerzell TJ, Esfandiary R, Joshi SB, Middaugh CR, Volkin DB. Protein–excipient interactions: mechanisms and biophysical characterization applied to protein formulation development. Adv Drug Deliv Rev. 2011;63(13):1118–59.
35. Ohtake S, Kita Y, Arakawa T. Interactions of formulation excipients with proteins in solution and in the dried state. Adv Drug Deliv Rev. 2011;63(13):1053–73.
36. Maity H, O'Dell C, Srivastava A, Goldstein J. Effects of arginine on photostability and thermal stability of IgG1 monoclonal antibodies. Curr Pharm Biotechnol. 2009;10(8):761–6.
37. Arakawa T, Timasheff S. The mechanism of action of Na glutamate, lysine HCl, and piperazine-N, N'-bis (2-ethanesulfonic acid) in the stabilization of tubulin and microtubule formation. J Biol Chem. 1984;259(8):4979–86.
38. Dion MZ, Leiske D, Sharma VK, de Zafra CLZ, Salisbury CM. Mitigation of oxidation in therapeutic antibody formulations: a biochemical efficacy and safety evaluation of N-acetyl-tryptophan and L-methionine. Pharm Res. 2018;35(11):222.
39. Arakawa T, Timasheff SN. Stabilization of protein structure by sugars. Biochemistry. 1982;21(25):6536–44.
40. Sudrik CM, Cloutier T, Mody N, Sathish HA, Trout BL. Understanding the role of preferential exclusion of sugars and polyols from native state IgG1 monoclonal antibodies and its effect on aggregation and reversible self-association. Pharm Res. 2019;36(8):109–9.
41. Amani M, Barzegar A, Mazani M. Osmolytic effect of sucrose on thermal denaturation of pea seedling copper amine oxidase. Protein J. 2017;36(2):147–53.
42. Oshima H, Kinoshita M. Effects of sugars on the thermal stability of a protein. The Journal of Chemical Physics. 2013;138(24):06B612_611.
43. Flood A, Estrada M, McAdams D, Ji Y, Chen D. Development of a freeze-dried, heat-stable influenza subunit vaccine formulation. PloS One. 2016;11(11).
44. Fischer S, Hoernschemeyer J, Mahler H-C. Glycation during storage and administration of monoclonal antibody formulations. Eur J Pharm Biopharm. 2008;70(1):42–50.
45. Ouellette D, Alessandri L, Piparia R, Aikhoje A, Chin A, Radziejewski C, et al. Elevated cleavage of human immunoglobulin gamma molecules containing a lambda light chain mediated by iron and histidine. Anal Biochem. 2009;389(2):107–17.

46. Adem YT, Molina P, Liu H, Patapoff TW, Sreedhara A, Esue O. Hexyl glucoside and hexyl maltoside inhibit light-induced oxidation of tryptophan. J Pharm Sci. 2014;103(2):409–16.
47. International Council for Harmonisation of Technical Requirements for Pharmaceuticals for Human Use. Guideline for elemental impurities Q3D (R1). 2019.
48. Baertschi SW, Clapham D, Foti C, Jansen PJ, Kristensen S, Reed RA, et al. Implications of in-use photostability: proposed guidance for photostability testing and labeling to support the administration of photosensitive pharmaceutical products, part 1: drug products administered by injection. J Pharm Sci. 2013;102(11):3888–99.
49. Cai H, Liu X, Zou J, Xiao J, Yuan B, Li F, et al. Multi-wavelength spectrophotometric determination of hydrogen peroxide in water with peroxidase-catalyzed oxidation of ABTS. Chemosphere. 2018;193:833–9.
50. Illes E, Patra SG, Marks V, Mizrahi A, Meyerstein D. The Fe(II)(citrate) Fenton reaction under physiological conditions. J Inorg Biochem. 2020;206:111018.
51. Li S-C, Goto NK, Williams KA, Deber CM. Alpha-helical, but not beta-sheet, propensity of proline is determined by peptide environment. Proc Natl Acad Sci. 1996;93(13):6676–81.
52. Bommana R, Mozziconacci O, Wang YJ, Schöneich C. An efficient and rapid method to monitor the oxidative degradation of protein pharmaceuticals: probing tyrosine oxidation with fluorogenic derivatization. Pharm Res. 2017;34(7):1428–43.
53. Hanlon MC, Seybert DW. The pH dependence of lipid peroxidation using water-soluble Azo initiators. Free Radic Biol Med. 1997;23(5):712–9.
54. Schoneich C, Aced A, Asmus KD. Halogenated peroxyl radicals as two-electron-transfer agents. Oxidation of organic sulfides to sulfoxides. J Am Chem Soc. 1991;113(1):375–6.
55. Davies MJ. The oxidative environment and protein damage. Biochim Biophys Acta. 2005;1703(2):93–109.
56. Sharma CP, Karim AV, Shriwastav A. Decolorization of methylene blue using Fe(III)-citrate complex in a solar photo-Fenton process: impact of solar variability on process optimization. Water Sci Technol. 2019;80(11):2047–57.
57. Marion A, Brigante M, Mailhot G. A new source of ammonia and carboxylic acids in cloud water: the first evidence of photochemical process involving an iron-amino acid complex. Atmos Environ. 2018;195:179–86.
58. Hawkins C, Davies M. EPR studies on the selectivity of hydroxyl radical attack on amino acids and peptides. Journal of the Chemical Society, Perkin Transactions 2. 1998(12):2617–2622.
59. Perrin DD. The Stability of Complexes of Ferric Ion and Amino-Acids. J Chem Soc. 1958(Sep):3125–3128.
60. Neubecker TA, Kirksey ST, Chellappa KL, Margerum DW. Amine Deprotonation in copper(iii)-peptide complexes. Inorg Chem. 1979;18(2):444–8.
61. Sysak PK, Foote CS, Ching TY. Chemistry of Singlet Oxygen .25. Photooxygenation of Methionine. Photochem Photobiol 1977;26(1):19–27, Chemistry of Singlet Oxygen—xxv. Photooxygenation of Methionine.
62. Hiller K, Masloch B, Goebl M, Asmus K. Mechanism of the hydroxyl radical induced oxidation of methionine in aqueous solution. J Am Chem Soc. 1981;103(10):2734–43.
63. Morelli R, Russo-Volpe S, Bruno N, Lo SR. Fenton-dependent damage to carbohydrates: free radical scavenging activity of some simple sugars. J Agric Food Chem. 2003;51(25):7418–25.
64. Barata-Vallejo S, Ferreri C, Postigo A, Chatgilialoglu C. Radiation chemical studies of methionine in aqueous solution: understanding the role of molecular oxygen. Chem Res Toxicol. 2010;23(1):258–63.
65. Enns K, Burgess WH. The photochemical oxidation of ethylenediaminetetraacetic acid and methionine by Riboflavin1. J Am Chem Soc. 1965;87(24):5766–70.
66. Udayakumar S, Ajaikumar S, Pandurangan A. Electrophilic substitution reaction of phenols with aldehydes: enhance the yield of bisphenols by HPA and supported HPA. Catal Commun. 2007;8(3):366–74.
67. Faith HE. Aldehyde-phenol reaction products and derivatives. J Am Chem Soc. 1950;72(2):837–9.
68. Asaduzzaman M, Scampicchio M, Biasioli F, Bremer PJ, Silcock P. Methanethiol formation during the photochemical oxidation of methionine-riboflavin system. Flavour and Fragrance Journal. 2020;35:34–41.
69. Sreedhara A, Wong RL, Lentz Y, Schoenhammer K, Stark C. Application of QbD principles to late-stage formulation development for biological liquid products. In. Quality by Design for Biopharmaceutical Drug Product Development: Springer; 2015. p. 115–135, Application of QbD Principles to Late-Stage Formulation Development for Biological Liquid Products.
70. Wurth C, Demeule B, Mahler H-C, Adler M. Quality by design approaches to formulation robustness—an antibody case study. J Pharm Sci. 2016;105(5):1667–75.
71. Walling C, Kurz M, Schugar HJ. Iron(Iii)-Ethylenediaminetetraacetic Acid-Peroxide System. Inorg Chem. 1970;9(4):931-&.
72. Rahhal S, Richter HW. Reduction of Hydrogen-Peroxide by the Ferrous Iron Chelate of Diethylenetriamine-N,N,N',N",N"-Pentaacetate. J Am Chem Soc 1988;110(10):3126–3133.
73. Li LX, Abe Y, Kanagawa K, Shoji T, Mashino T, Mochizuki M, et al. Iron-chelating agents never suppress Fenton reaction but participate in quenching spin-trapped radicals. Anal Chim Acta. 2007;599(2):315–9.
74. Brausam A, van Eldik R. Further mechanistic information on the reaction between Fe-III(edta) and hydrogen peroxide: observation of a second reaction step and importance of pH. Inorg Chem. 2004;43(17):5351–9.
75. Rachmilovich-Calis S, Masarwa A, Meyerstein N, Meyerstein D, van Eldik R. New mechanistic aspects of the Fenton reaction. Chem-Eur J. 2009;15(33):8303–9.
76. Graf E, Mahoney JR, Bryant RG, Eaton JW. Iron-catalyzed hydroxyl radical formation. Stringent requirement for free iron coordination site. J Biol Chem. 1984;259(6):3620–4.